Figure S1

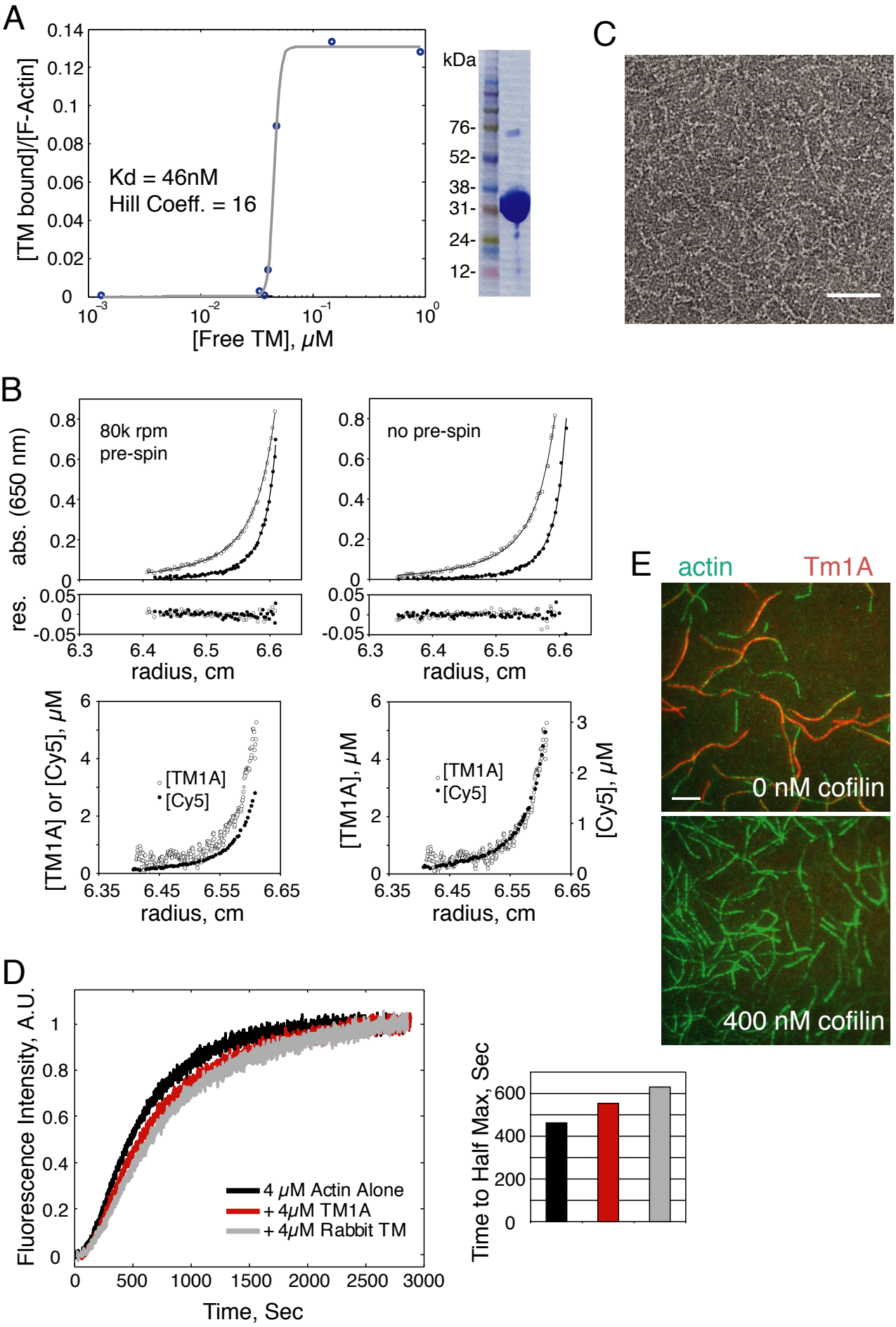
A
[TM bound]/[F-Actin]
Kd = 46nM
Hill Coeff. = 16
[Free TM], μM
kDa
76-
52-
38-
31-
24-
12-
C
B
80k rpm
pre-spin
no pre-spin
abs. (650 nm)
res.
radius, cm
[TM1A] or [Cy5], μM
[TM1A]
[Cy5]
[TM1A], μM
[Cy5], μM
E
actin
Tm1A
0 nM cofilin
400 nM cofilin
D
Fluorescence Intensity, A.U.
4 μM Actin Alone
+ 4μM TM1A
+ 4μM Rabbit TM
Time, Sec
Time to Half Max, Sec

Figure S2

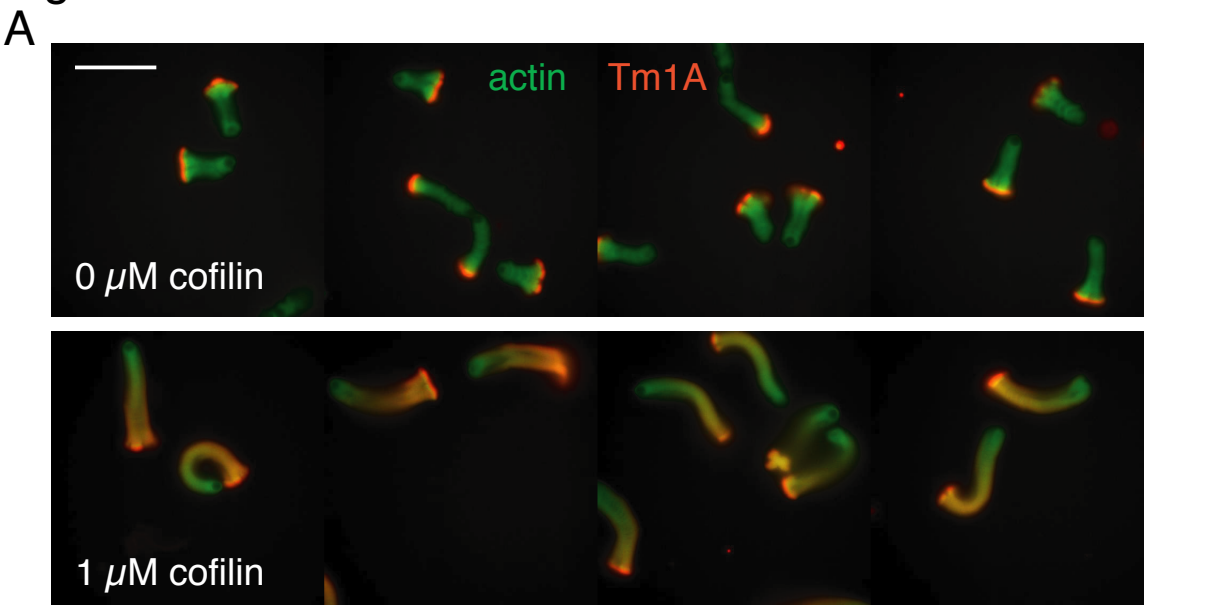
A
actin
Tm1A
0 μM cofilin
1 μM cofilin

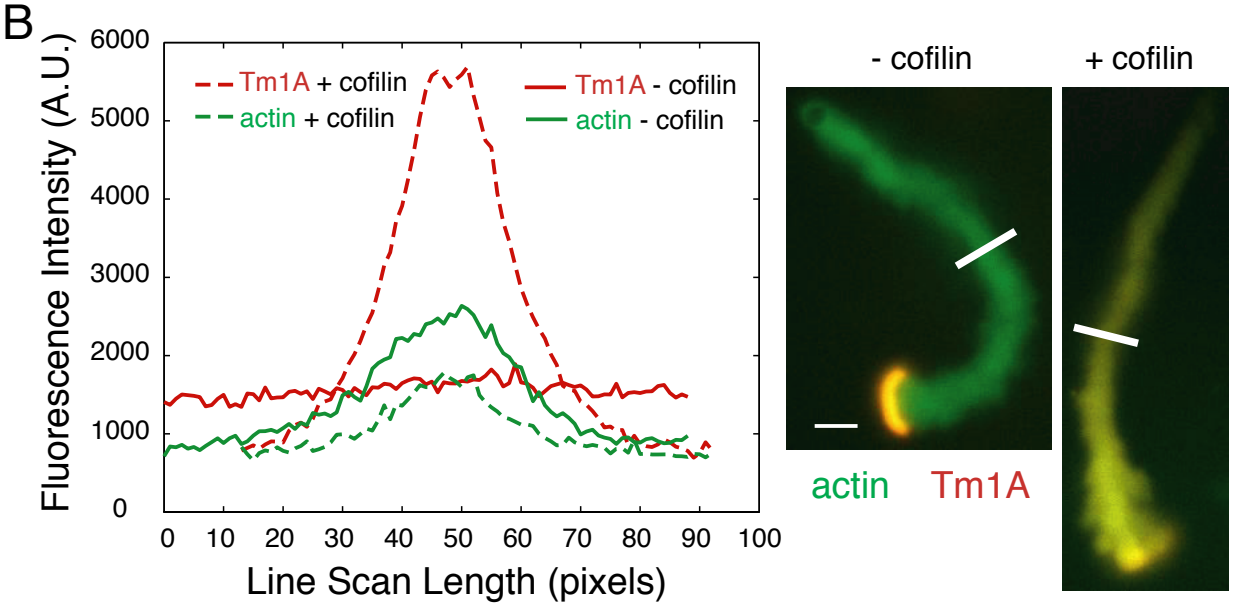
B
Fluorescence Intensity (A.U.)
Tm1A + cofilin
actin + cofilin
Tm1A - cofilin
actin - cofilin
Line Scan Length (pixels)
- cofilin
+ cofilin
actin
Tm1A

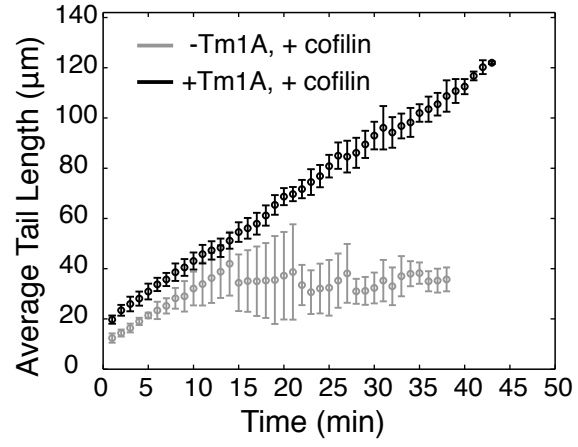
C
Average Tail Length (μm)
-Tm1A, + cofilin
+Tm1A, + cofilin
Time (min)

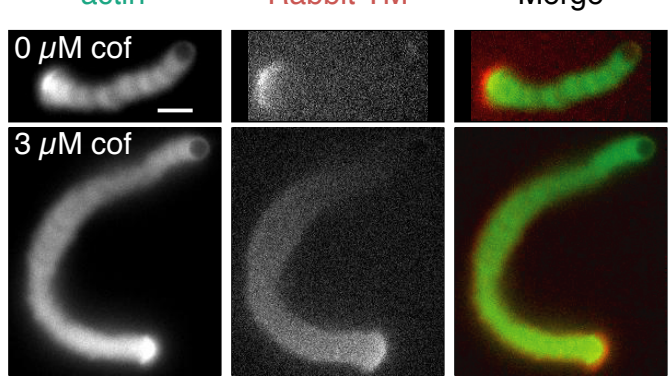
D
actin
Rabbit TM
Merge
0 μM cof
3 μM cof

Figure S3

A

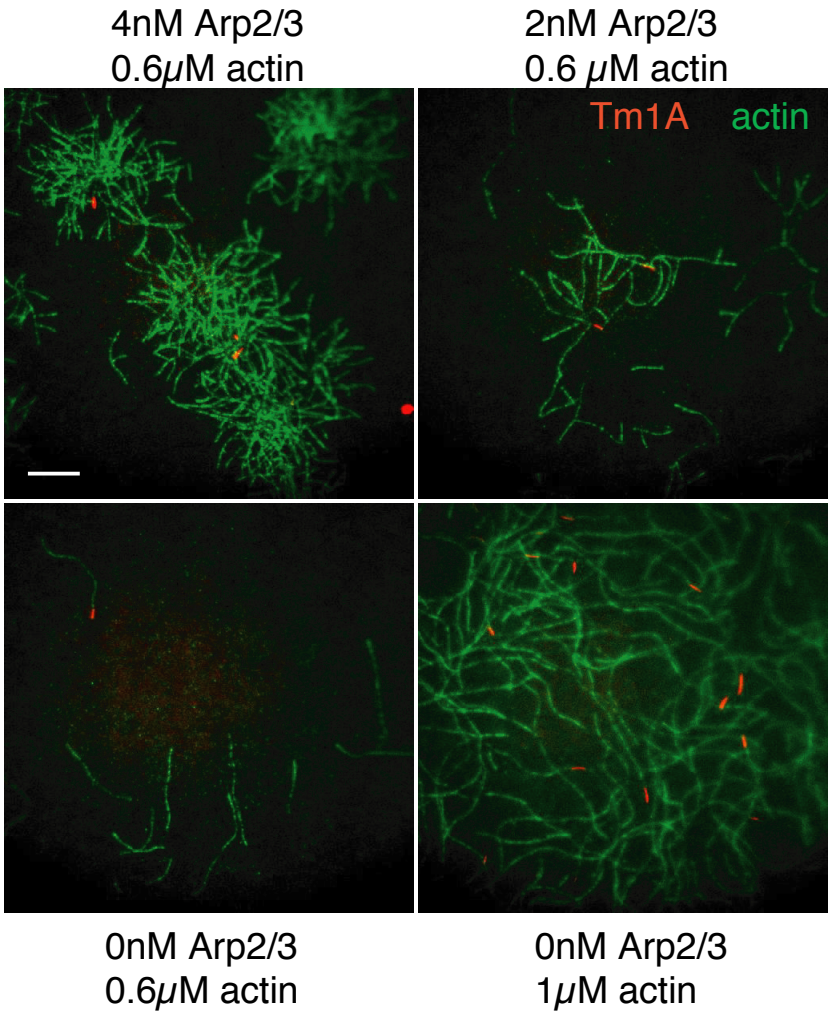
4nM Arp2/3
0.6μM actin
2nM Arp2/3
0.6 μM actin
Tm1A
actin
0nM Arp2/3
0.6μM actin
0nM Arp2/3
1μM actin

Figure S4

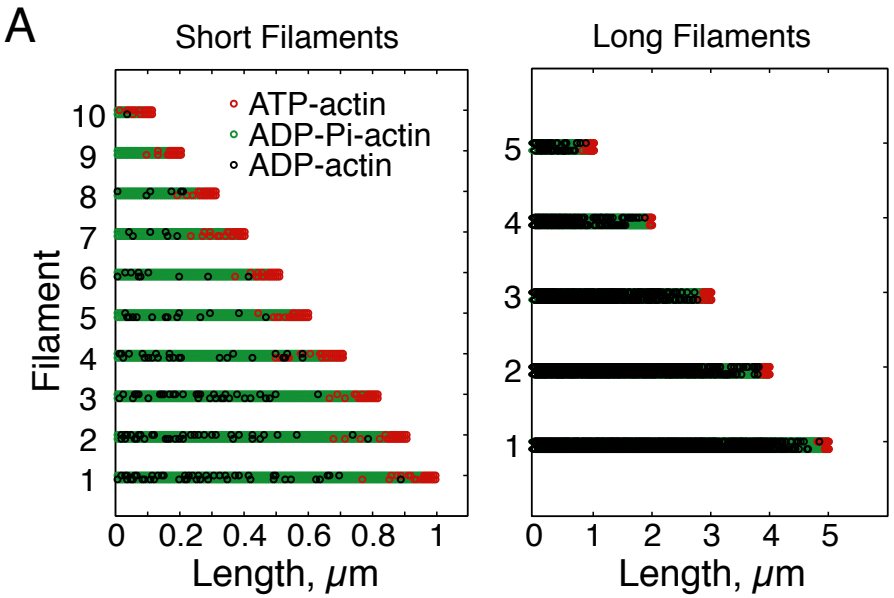
A
Short Filaments
Long Filaments
ATP-actin
ADP-Pi-actin
ADP-actin
Filament
Length, μm
Length, μm

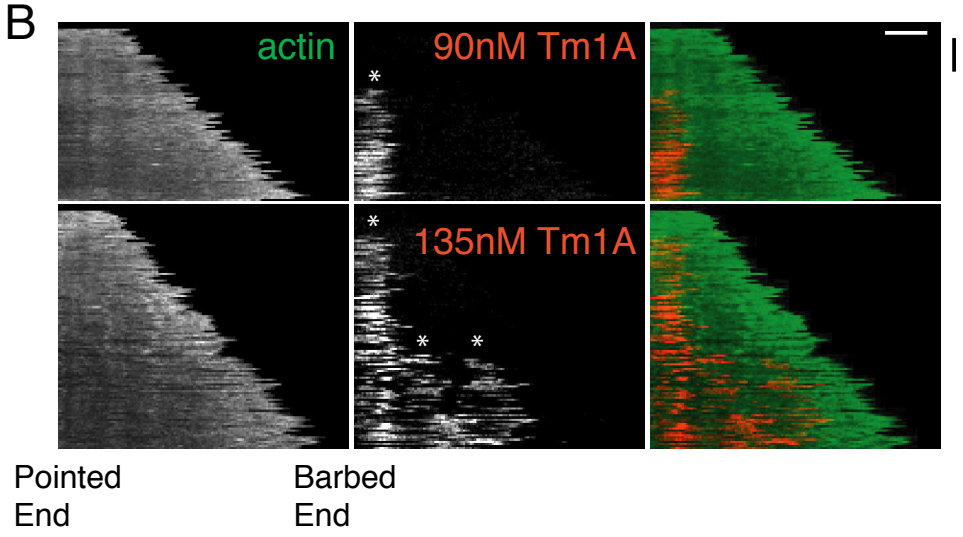
B
actin
90nM Tm1A
135nM Tm1A
Pointed End
Barbed End

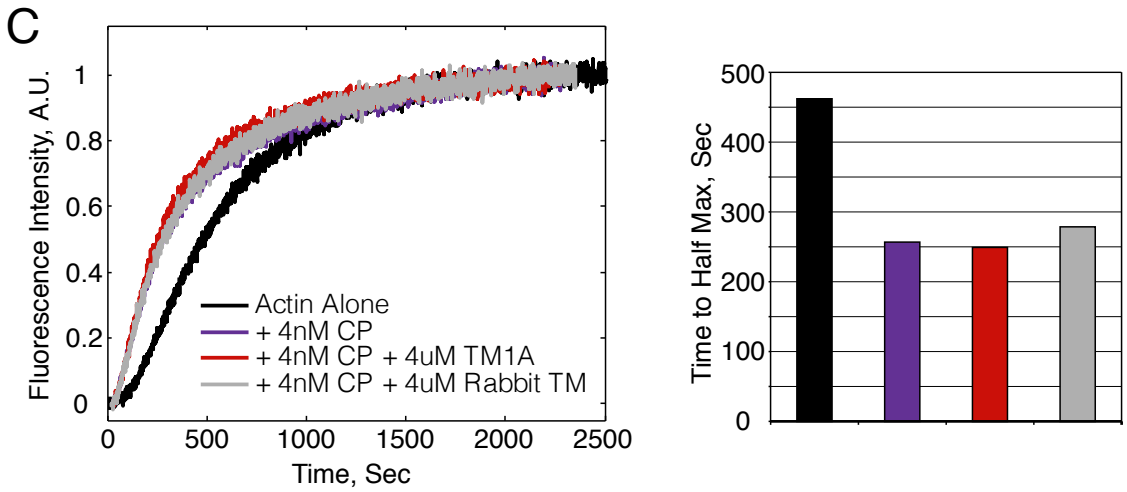
C
Fluorescence Intensity, A.U.
Time, Sec
Actin Alone
+ 4nM CP
+ 4nM CP + 4uM TM1A
+ 4nM CP + 4uM Rabbit TM
Time to Half Max, Sec

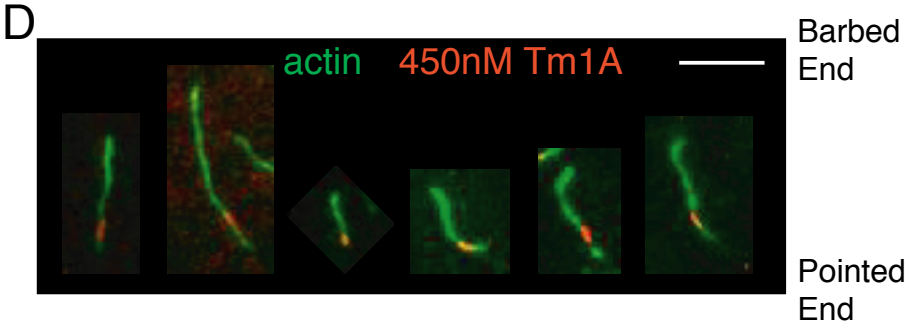
D
actin
450nM Tm1A
Barbed End
Pointed End

Figure S5

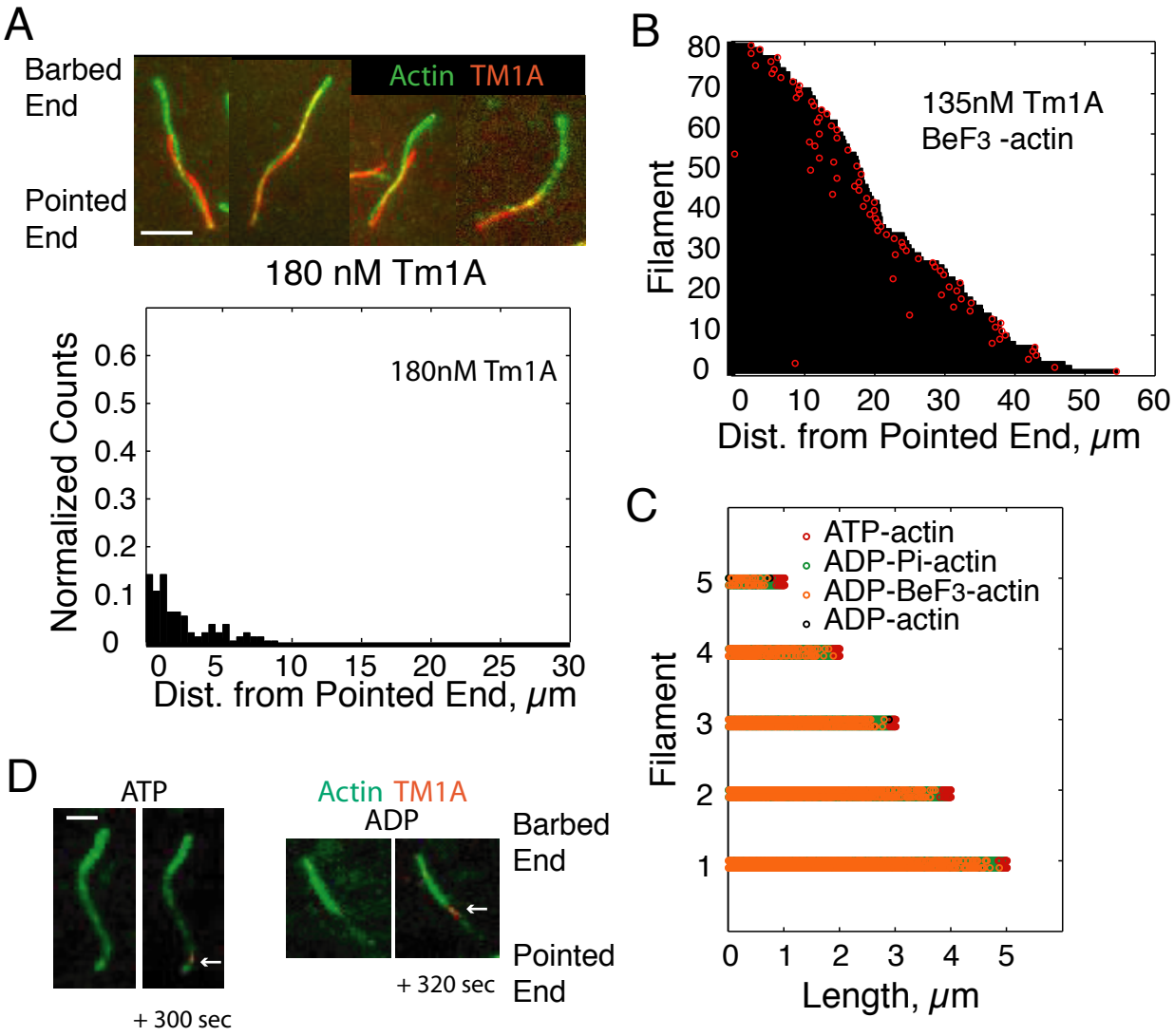
A
Barbed End
Pointed End
Actin TM1A
180 nM Tm1A
Normalized Counts
180nM Tm1A
Dist. from Pointed End, μm
B
135nM Tm1A
BeF3 -actin
Filament
Dist. from Pointed End, μm
C
ATP-actin
ADP-Pi-actin
ADP-BeF3-actin
ADP-actin
Filament
Length, μm
D
ATP
+ 300 sec
Actin TM1A
ADP
+ 320 sec
Barbed End
Pointed End

Supplemental Figure Captions

Figure S1 (Supplemental to Figure 1). (A) Co-pelleting of Tm1A with actin filaments. Kd = 46nM, Hill Coefficient = 16. Right: SDS-page gel of purified Tm1A. (B) Analytical ultracentrifugation of Cy5-labeled Tm1A shows that the concentration is 45μM with a labeling percentage of 65%. Without pre-spinning the protein, there is a population of molecules with a larger mass than a Tm1A dimer. (C) Electron micrograph of 4.5μM Cy5-labeled Tm1A shows that the larger mass particles in (b) are in fact small polymers and are not aggregate protein. (D) Tm1A has a negligible effect on spontaneous nucleation and elongation of actin filaments. Time-resolved pyrene fluorescence of polymerizing actin filaments in the absence and presence of Tm1A and RSK muscle TM. Right: Bar graph of time to half max. (E) Cofilin and Tm1A binding are mutually exclusive. Green: Alexa488-labeled actin. Red: Cy5-labeled Tm1A. Top: 5% 1μM A488-actin, 180nM Cy5-Tm1A. Bottom: 5% 0.8μM A488-actin, 180nM Cy5-Tm1A, 400nM cofilin.

Figure S2 (Supplemental to Figure 2). (A) Actin networks generated from ActA-coated polystyrene microspheres by the Arp2/3 complex and capping protein exclude tropomyosin in the absence of cofilin. Cofilin renders dendritic actin networks competent to bind tropomyosin. Four random fields taken 30min into the reaction show that the effect is robust. Green: Alexa488-labeled actin. Red: Cy3-labeled Tm1A. Each row has the indicated concentration of cofilin. Scale bar: 40μm. (B) Dendritic actin networks imaged 2 hours after the reaction began show that in the absence of cofilin, Tm1A does not bind into the network. Scale bar: 10μm. Left: Fluorescence intensity line scans of the networks from the right. Solid lines: without cofilin. Dotted lines: with cofilin. (C) Graph of actin network length versus time in the presence and absence of Tm1A. (D) Rabbit skeletal muscle (RSK) TM also requires the activity of cofilin to bind motile

actin networks generated by the Arp2/3 complex and capping protein. Left: fluorescence of Alexa488-labeled actin. Middle: Cy3-labeled RSK TM. Right: merge of actin and RSK TM fluorescence. Scale bar: 10μm.

Figure S3 (Supplemental to Figure 3). (A) In the presence of Arp2/3 complex, Tm1A only binds to free pointed ends and is blocked by Arp2/3-bound pointed ends. Controls in single filament TIRF showing that when we increase the number of free pointed ends in the absence of Arp2/3 complex, the number of Tm1A-bound pointed ends increases. However, if the number of pointed ends is increased by adding Arp2/3 complex, the number of Tm1A-bound pointed ends does not increase. Green: Alexa488-labeled actin. Red: 90nM Cy5-labeled Tm1A. Top panels: Left: 4nM Arp2/3, 40nM ActA, 600nM A488-actin; Right: 2nM Arp2/3, 40nM ActA, 600nM A488-actin. Bottom panels: 0nM Arp2/3; Left: 600nM A488-actin; Right: 1μM A488-actin.

Figure S4 (Supplemental to Figure 4). (A) Simulation of the ATP state of subunits in growing actin filaments. Left: filaments frozen at 0.1μm intervals. Right: filaments frozen at 1μm intervals. (B) Hand-drawn kymographs of Tm1A binding and spreading along actin filaments. Top panel: 90nM Cy5-Tm1A. Bottom panel: 135nM Cy5-Tm1A. White scale bar: 10μm. Black time bar: 500 sec. (C) Tm1A has a negligible effect on CP induced nucleation and pointed-end elongation of actin filaments. Time-resolved pyrene fluorescence of polymerizing actin filaments in the absence and presence of Tm1A and RSK muscle TM. Right: Bar graph of time to half max. (D) Filaments attached to the coverslip surface show that Tm1A often binds “near” the pointed end, but not necessarily “at” the pointed end. 600nM A488-actin, 450nM Cy5-Tm1A.

Figure S5 (Supplemental to Figure 5). (A) Tm1A binds to the pointed end of actin filaments in single filament TIRF. Red: 180nM Cy5-Tm1A. Green: 600nM A488-actin. Scale bar: 5μm. Bottom panel: Normalized histograms of Tm1A binding events as a function of the distance from the pointed end of actin filaments (115 binding events). (B) Tm1A binds to the barbed end of actin filaments formed in the presence of BeF3. Visual representation of each binding event of 135nM Cy5-Tm1A to BeF3-actin filaments. (C) Simulation of the ATP state and BeF3 binding to subunits in growing actin filaments. Filaments are frozen at 1μm intervals. (D) Polarization-marked filaments allow us to determine binding of Tm1A to ATP-actin vs. ADP-actin. 10% A488-actin marks the pointed end while 30% A488-actin marks the barbed end. Arrows point to Tm1A binding events.

Supplemental Materials and Methods

Design of labeled tropomyosin.

For *in vitro* biochemical experiments we constructed a recombinant version of the Tm1A isoform of *Drosophila* tropomyosin. We labeled our engineered protein with Cy3- or Cy5-maleimide to produce Cy3-Tm1A and Cy5-Tm1A.

We designed our labeled tropomyosin so that the label would be least disruptive to the protein's structure and function. The two regions of the protein we avoided placing a cysteine for labeling were: i. the coiled-coil dimerization interface, and ii. the actin binding regions of the protein [S1, S2, S3]. To identify the actin binding regions, we searched for the motif: K/R, X, X, X, N ,X, E, X, X, X, E/D, K/R, A/Y, X, D/E, X, A, X, N, A/S. For Tm1A, we replaced the endogenous cysteine with an alanine, C32A. By following the two principles above, we then chose a serine to replace with a cysteine, S82C. Since Tm1A is acetylated *in vivo* (Goins and Mullins, in press), we also genetically encoded an acetylation mimic to the N terminus of the protein: AS-Tm1A. An AS fused to the N terminus of skeletal TM expressed in E. coli has previously been shown to replace the function of the N-acetyl group, both in regulatory function and actin binding affinity [S4]. The first amino acids in our Tm1A construct are MASMTTS.

We determined the concentration of Tm1A stock solutions as well as the efficiency of fluorescent labeling by analytical ultracentrifugation (Cy5-Tm1A: 45μM, 65% labeled; Cy3-Tm1A: 50μM, 70% labeled; Figure S1B). Analytical ultracentrifugation also revealed that, at micromolar concentrations, Tm1A forms dimers that are in equilibrium with a small fraction of higher molecular weight species. By electron microscopy these higher molecular weight species appear to be head-to-tail polymers rather than non-specific aggregates (Figure S1C).

Protein Purification & Labeling

Rabbit Skeletal Muscle Actin

Actin was purified from rabbit acetone powder by the method of Supich and Watt (1971) [S5]. Briefly, rabbit muscle acetone powder (Pel-Freeze) was resuspended in G buffer (0.5 mM TCEP, 0.1 mM $CaCl_2$, 0.2mM ATP, 2mM Tris pH 8.0) and let to stir on ice for 30min. The acetone powder was pelleted by centrifugation at 30k rcf for 30 min. The supernatant was filtered through cheesecloth. The actin was polymerized by adding KCl and MgCl2 to 50mM and 2mM, respectively. Polymerization occurred at RT for 15min, and continued on ice for 15 min. KCl was added to 0.8M, and allowed to stir at 4°C for 15 min to dissociate tropomyosin. Actin was pelleted in a Ti45 rotor for 2hrs at 142k rcf. The pellet was resuspended in G buffer and dounced before dialysis into G buffer for 2-3 days. Actin was gel filtered and stored in G buffer at 4°C.

Actin Labeling

Rabbit skeletal muscle actin was labeled on Cys-374 with pyrene-iodoacetamide (Invitrogen), as described [S6]. Briefly, gel-filtered Rabbit Skeletal Muscle actin was diluted to around 1mg/ml (27μM) and polymerized by addition of KMEI (50 mM KCl, 1 mM $MgCl_2$, 1 mM EGTA, 10 mM imidazole pH 7.0). Polymerized actin was dialyzed against L-KMEI (100 mM KCl, 2 mM $MgCl_2$, 25 mM imidazole pH 7.5, 0.3 mM ATP). Actin was transferred to a small beaker and 4-7 moles of pyrene-iodoacetamide (Invitrogen) per mole of actin, were added while stirring. The reaction was covered with foil and allowed to proceed overnight, with gentle stirring. The reaction was quenched with 10mM DTT and precipitated dye was removed by low speed centrifugation at 4k rcf. Labeled actin filaments were pelleted by centrifugation for 2 hours at 142k rcf in a Type 45 Ti Rotor (Beckman-Coulter). Filamentous labeled actin was depolymerized by

dialyzing into Buffer A (2mM Tris HCl, pH 8.0, 0.2mM ATP, 0.1mM $CaCl_2$, 0.5mM TCEP, 0.04% azide) and gel filtered on an S75 column (GE Healthcare). Labeled actin was stored at 4°C in the dark.

Actin was labeled with Alexa-488 maleimide (Invitrogen) while in the de-polymerized state. Briefly, G-Actin was dialyzed overnight into L-Buffer A (5 mM Tris pH 8.0, 0.2 mM ATP, 0.1 mM $CaCl_2$). 5 molar excess of Alexa-488 maleimide was added to the actin. The reaction proceeded on ice for 15 minutes and was quenched with 10mM DTT. Actin was polymerized by addition of 1X KMEI (50 mM KCl, 1 mM $MgCl_2$, 1 mM EGTA, 10 mM imidazole pH 7.0). Filamentous, labeled actin was collected by centrifugation, and both resuspended in and dialyzed against Buffer A to depolymerize. Labeled actin was gel filtered on an S75 column (GE Healthcare).

AS-Tm1A

The AS-Tm1A C32A/S82C construct, in a pET20b vector, was expressed in BL21 E. coli cells. Bacterial pellets were resuspended in a 3X volume of lysis buffer (50 mM Tris pH 7.5, 10 mM EDTA, 2 mM DTT, 200mM NaCl, 1 mM PMSF, 5 mg/L DNAse1, 10 mg/L RNAseA) and lysed by passage through a microfluidizer and cleared by centrifugation. The supernatant, in a 50 ml conical tube, was placed in a boiling water bath (95°C) for 7 min (or until the supernatant precipitates), then placed in RT water for 7 min, then on ice for 30 min. The precipitate was pelleted by centrifugation at 150k rcf, 4°C for 45 min, and the supernatant recovered. Precipitate the tropomyosin by adding 1N HCl until the pH is below the PI (4.69). The precipitate was pelleted by centrifugation at 20k rcf, 4°C for 20 min. The pellet was resuspended in 20mM Tris-HCl pH 7.5, 0.5mM TCEP, and KOH added until the pH returned to 7.5. A 20-40% ammonium sulfate

cut was taken from the resuspended pellet, and centrifuged at 130k rcf for 20 min at 4°C. The pellet was resuspended in and dialyzed into 10mM imidazole pH 7, 100mM KCl, 0.5mM TCEP. The purified protein was flash frozen and stored at -80°C. The concentration of this protein was determined using a quantitative NuPAGE 4-12% Bis-Tris gel, stained with Sypro-Red stain (Life Technologies), and imaged on a GE Healthcare Typhoon imager. A titration of actin concentrations was used as a standard.

Rabbit Skeletal TM

Rabbit skeletal tropomyosin was purified from rabbit acetone powder by the method of Smillie (1982) [S7]. Briefly, rabbit muscle acetone powder (Pel-Freeze) was resuspended in extraction buffer (25mM Tris pH 8.0, 1M KCl, 0.1 mM $CaCl_2$, 0.2mM ATP, 0.5 mM DTT) and let to stir at RT for 16hrs. The acetone powder was filtered out with cheesecloth, and the filtrate cleared by centrifugation at 20k rcf for 10 min at 4°C. Precipitate the tropomyosin by adding 1N HCl until the pH is below the PI (4.69). The precipitate was pelleted by centrifugation at 20k rcf, 4°C for 10 min. The pellet was resuspended in 1M KCl, 0.5mM DTT, and the pH adjusted to 7.4 by addition of 1N KOH. The solution was clarified by centrifugation at 20k rcf, 4°C for 10 min. A 25-35% ammonium sulfate cut was taken from the supernatant, and centrifuged at 20k rcf for 10 min at 4°C. The pellet was resuspended in and dialyzed into 25mM imidazole pH 7.4, 100mM KCl, 2mM $MgCl_2$, 1mM EGTA, 1mM β-ME. The purified protein was flash frozen and stored at -80°C.

TM Labeling

The D. melangaster tropomyosin isoform was labeled on an engineered cysteine (AS-Tm1A C32A/S82C). The rabbit tropomyosin was labeled on the native cysteines (alpha TM: C190, beta TM: C36). Each isoform was first pre-reduced in 5mM TCEP, 10mM Imidazole pH 7.0, 100mM KCl for 10min. The protein was then buffer exchanged into 10mM Imidazole pH 7.0, 100mM KCl with a pre-equilibrated PD-10. AlexaFluor 488, Cy3-MonoMaleimide, or Cy5-MonoMaleimide (all Sigma) was added to 4 times above the molar concentration of protein, and allowed to incubate on ice for 30min. Any aggregate label was removed by centrifugation at 230k rcf, 4°C for 20min. Free label was removed by buffer exchanging into 10mM imidazole pH 7, 100mM KCl, 0.5mM TCEP. The labeled protein was flash frozen and stored at -80°C.

Capping Protein

Recombinant mouse capping protein CPα1β2 was purified as described in Palmgren et al. (2001) [S8]. Briefly, the protein construct, in a pET3d vector, was expressed in BL21 E. coli cells. Bacterial pellets were resuspended in a 3X volume of lysis buffer (50mM Tris pH 8.0, 1mM EDTA, 1mM DTT, 1mM PMSF) and lysed by passage through a microfluidizer and cleared by centrifugation. A 50-70% ammonium sulfate cut was taken from the cleared lysate and centrifuged at 32k rcf for 20 min at 4°C. The pellet was resuspended in 20mL of HA dialysis buffer (1mM NaH_2PO_4 pH 7.0, 1mM DTT) and dialyzed overnight into the same buffer with at least three changes. The dialysate was loaded onto an HA column (GE Healthcare) with 10mM NaH_2PO_4 pH 7.0, and then eluted with a gradient from 10-250mM NaH_2PO_4. Peak fractions were pooled and dialyzed against QA dialysis buffer (10mM Tris pH 8.0, 10mM KCl, 0.5mM EDTA, 0.5mM TCEP). The sample was loaded onto a MonoQ column (GE Healthcare) and eluted with

a 10-400mM KCl gradient. Selected fractions were dialyzed into SA dialysis buffer (10mM MES pH 5.8, 0.5mM EDTA, 1mM DTT). The sample was loaded onto a MonoS column (GE Healthcare) and eluted with a 0-350mM NaCl gradient. Selected fractions were dialyzed into storage buffer (10mM Tris pH 8.0, 40mM KCl, 0.5mM TCEP, 50% glycerol), flash frozen, and stored at -80°C.

Ancanthamoeba castellani Arp2/3 Complex

Arp2/3 was prepared from Acanthamoeba castellini by the method of Dayel et al. (2001) [S9]. Briefly, 15L of Ancanthamoeba castellani were grown up, harvested and washed into 10mM Tris, pH 8.0 at 4°C, 100mM NaCl. The cells were ruptured by release from a Parr bomb equilibrated wtih nitrogen at 400 p.s.i. Lysate was cleared with centrifugation first at a low speed, 15 min, 4k rcf at 4°C; then at a higher speed, 2 hrs, 113k rcf at 4°C. After centrifugation, the top layer of lipids was removed by gentle aspiration, and the pellet discarded. The lysate was loaded onto a DEAE column, and the flow through collected. The flow through was then loaded onto an NWASP WWCA-Sepharose column, washed with 10mM Tris pH 8.0, 50mM NaCl, 0.1mM $CaCl_2$, 0.2mM ATP, 1mM DTT, 15 ug/mL Benzamidine. The protein complex was eluted with 10mM Tris pH 8.0, 400mM $MgCl_2$, 1mM DTT, and dialyzed into MonoS low buffer (10mM Tris pH 8.0, 0.5mM TCEP, 0.5mM $MgCl_2$, 0.1mM ATP). The sample was loaded onto a MonoS column (GE Healthcare) and eluted with a 0-500mM NaCl gradient. Selected fractions were gel filtered using a Superdex 200 column (GE Healthcare) into 20mM HEPES pH 7.0, 0.5mM TCEP, 25mM KCl, 0.2mM $MgCl_2$, 0.1mM ATP. Glycerol was added to 10% and the purified protein flash frozen and stored at -80°C.

ActA$^{30\text{-}612}$-KCK-6XHis

ActA$^{30\text{-}612}$-KCK-6XHis was purified as described in Akin and Mullins (2008) [S10]. Briefly, the construct, cloned in a pET 17b vector, was expressed in BL21 E. coli cells. Bacterial pellets were resuspended in 4-5X volume of lysis buffer (100mM NaH_2PO_4 pH 8.0, 10mM Tris base, 6M Guanidium HCl, 10mM 2-mercaptoethanol, 1mM PMSF) and lysed by nutating overnight at room temperature. Clarified lysate was batch bound to Ni-NTA resin (1-2mL of resin per liter of culture) for 30 min. The resin was washed with wash buffer (100mM NaH_2PO_4 pH 7.8, 10mM Tris base, 10mM Imidazole, 6M Guanidium HCl, 10mM 2-mercaptoethanol), and eluted with elution buffer (100mM NaH_2PO_4 pH 7.5, 10mM Tris base, 250mM Imidazole, 6M Guanidium HCl, 10mM 2-mercaptoethanol). The eluate was dialyzed into Buffer QA (10mM Bistris-propane pH 7.0, 1mM EDTA, 0.5mM TCEP), loaded onto a MonoQ column (GE Healthcare) and eluted with a 100-300mM KCl gradient. Selected fractions were dialyzed into storage buffer (10mM HEPES pH 7.0, 50mM KCl, 1mM TCEP), flash frozen, and stored at -80°C.

Profilin 1

Recombinant human Profilin1 was purified, as described in Reichstein and Korn (1979) [S11], with the following modifications. The Profilin1, in vector pET16B, was expressed in E. coli BL21 pLysS. Bacterial cell pellets were resuspended in lysis buffer (10 mM Tris pH 8.0, 1 mM EDTA, 2 mM DTT, 1 mM PMSF) and lysed using an Emulsiflex. Ammonium sulfate was added to the clarified lysate to a concentration of 35%. After centrifugation, an additional 26% ammonium sulfate to a final concentration of 61% was added to the supernatant. After centrifugation, the pellet was resuspended in lysis buffer and dialyzed overnight against more lysis buffer. Protein was applied to a DEAE column and the flow through and wash fractions were collect-

ed. These fractions were dialyzed against HA Buffer (5mM K_2HPO_4 pH 7.5, 1mM DTT) and applied to a hydroxyapatite column. Flow through and wash fractions were pooled, and gel filtered (10mM Tris pH 7.5, 50mM NaCl, 0.5mM TCEP) using a Superdex 200 column connected to an ÄKTA Purifier system. Glycerol was added to 20% final concentration to the peak fractions. Protein was flash frozen in liquid nitrogen and stored at -80°C.

hCofilin 1

Recombinant human Cofilin1 was purified as described in Carlier et al. (1997) [S12], with the following modifications. The construct, cloned into a pET16b vector, was expressed in BL21 Rosetta cells (Novagen). E. coli lysate was dialyzed into DEAE buffer (10 mM Tris pH 7.8, 50 mM NaCl, 0.2 mM EDTA, 2 mM DTT, 1 mM PMSF). The flow through and wash from the DEAE column was dialyzed into (10 mM PIPES pH 6.5, 15 mM NaCl, 2 mM DTT, 0.2 mM EDTA), and loaded onto a MonoS 5/50 GL column connected to an ÄKTA Purifier system (GE Healthcare). Protein was gel filtered using a Superdex 200 column into 10 mM Tris pH 7.5, 50 mM NaCl, 0.5 mM TCEP; glycerol was added to 20% to peak fractions and protein was flash frozen and stored at -80°C.

Analytical Ultracentrifugation

For equilibrium sedimentation analysis, we first transferred full-length, Cy5-labeled Tm1A into fresh assay buffer (100 mM KCl, 0.5mM TCEP, 10 mM Imidazole pH 7.0) using a pre-equilibrated column of Sephadex G-25 resin (Nap5 column, GE Healthcare, Piscataway, NJ). We then diluted labeled protein to absorbance values of 0.15 cm^{-1}, 0.3 cm^{-1}, and 0.6 cm^{-1} at 650 nm. We loaded the three concentrations of labeled Tm1A, together with buffer-only blanks, into a

six-channel, charcoal-filled epon centerpiece housed in an equilibrium sedimentation cell (Beckman Coulter, Indianapolis, IN). We placed the sample cell into a four-hole analytical rotor (model An-60ti, Beckman Coulter) and spun the samples to equilibrium at three different speeds (10000, 14000, and 20000 rpm) in an analytical ultracentrifuge equipped with both absorbance and interference optics (model XL-I, Beckman Coulter). Every hour, until the samples reached equilibrium, we acquired radial absorbance scans at 650 nm. We also measured interference fringe displacements and used them to determine radial changes in the index of refraction along the cell. From the measured change in index of refraction, we computed the protein concentration profile at equilibrium [S13, S14]. Using the extinction coefficient of Cy5 (150,000 M^{-1} cm^{-1}) we converted radial absorbance at 650 nm into the dye concentration profile. Comparing the two calibrated curves revealed the efficiency of the dye labeling reaction. Finally, to determine the molecular weight of the Tm1A constructs, we fit equilibrium fringe displacement and absorbance profiles using multi-species models (both interacting and non-interacting). For this analysis, we performed global, nonlinear, least-squares fitting of data collected at three different protein concentrations and three different rotor speeds (9 data sets total), using two types of software: Sedphat (Peter Schuck, NIBIB/NIH) and Winnonln (David Yphantis, University of Connecticut, Storrs, CT).

Microscopy

Glass Chamber Treatment & Assembly

The same glass treatment and chamber assembly was used for both Bead Motility assays and Single Filament TIRF assays. To minimize non-specific protein absorption, glass slides were washed in ethanol and KOH. Glass coverslips were first washed in ethanol and KOH, and then

fully cleaned with plasma glow discharge. The coverslips were then treated with a 2.5% solution of APTES (3-Aminopropyltriethoxysilane from Sigma) in 5% water, 95% ethanol pH 4.5 (with acetic acid). After rinsing in ethanol and water, the coverslips were treated with 10% NHS-PEG(5000)-Biotin and 90% NHS-PEG(5000) in DMF. Microscopy chambers were assembled with double-stick tape between the slide and coverslip.

Bead Motility Assay

Carboxylated, polystyrene, 5µm diameter beads (Bangs Labs) were coated with $ActA^{30-612}$-KCK-6XHis using EDC-SulfoNHS chemistry, as described in Akin and Mullins (2008) [S10]. Coated beads were stored in 1mg/mL BSA, 2mM Tris pH 8.0 and used at 1:120 dilution in motility assays.

For motility assays without recycling agents (cofilin and profilin), we mixed the ActA-coated beads with 7.4µM 3% Alexa488 labeled actin, 210nM capping protein, 125nM Arp2/3, and varying amounts of labeled Tm1A. All assays were carried out in 0.2% methyl cellulose (400 cP), 2.5mg/mL BSA, 1mM $MgCl_2$, 1mM EGTA, 20mM HEPES pH 7.0, 50mM KOH [pH 7.0 with 15mM TCEP HCl], and 250µM ATP. For motility assays with recycling agents, we included the indicated concentration of hCofilin1, and added an equal concentration of hProfilin1.

All images were acquired at room temperature on a software-controlled (MicroManager) Nikon Eclipse TE2000-E inverted epifluorescence microscope equipped with an EM CCD camera (Andor iXon), and a Nikon 60X water immersion objective. After flowing in 10µL of the motility mix, glass chambers were sealed with VALAP (molten mixture of Vaseline, lanolin, and paraffin at 1:1:1 mass ratio), and imaged immediately. Images were taken at 60 second intervals.

Single Filament TIRF

All images were acquired at room temperature on a software-controlled (NIS Elements 4.1) Nikon Ti-E inverted TIRF microscope equipped with an EM CCD camera (Andor DU897), and a Nikon 100X oil immersion objective. Each chamber was initially incubated for 1 min with blocking solution (10mM Imidazole, pH 7.0, 50mM KCl, 1mM $MgCl_2$, 1mM EGTA, 1mg/mL BSA, 1% Pluronic acid, 250 μg/mL κ-casein). The chamber was then rinsed with 1X KMEI/BSA (10mM Imidazole, pH 7.0, 50mM KCl, 1mM $MgCl_2$, 1mM EGTA, 1mg/mL BSA). For assays where the filaments were not attached to the coverslip, the protein mix (labeled actin, tropomyosin, Arp2/3, hcofilin1 in 0.2% methyl cellulose (400cP), 1mg/mL BSA, 1mM $MgCl_2$, 1mM EGTA, 50mM KCl, 200μM ATP, 20mM glucose, 250μg/mL glucose oxidase, 50μg/mL catalase, 20mM βME, and 10mM Imidazole, pH 7.0) was flowed in, then the chamber sealed with VALAP (molten mixture of Vaseline, lanolin, and paraffin at 1:1:1 mass ratio), and imaged immediately. For assays where the filaments were attached, before flowing in the protein mix, the chamber was treated with 1μM Streptavidin, rinsed with 1X KMEI/BSA, then 1μM biotin-phalloidin, and rinsed with 1X KMEI/BSA. For assays with BeF_3, 1mM $BeCl_2$ and 5mM KF were added to the protein mix before starting the reaction. Images were taken at 10 second intervals.

TIRF binding assay

To determine the binding affinity of Tm1A for actin using single filament TIRF, 20% 200nM A488-actin with varying amounts of Cy5-Tm1A (5-160nM) were sealed in glass chambers with VALAP and allowed to incubate in the dark at room temperature for 3.5 hrs to reach steady state. 2-color images of 20 random fields were taken for each concentration of Tm1A.

TIRF with Cofilin

To examine Tm1A's ability to protect actin filaments from cofilin severing, the chambers were first incubated with 1μM streptavidin and 1μM biotin-phalloidin so the actin filaments would be attached to the coverslip. A single filament TIRF reaction with 20% 600nM A488-actin with or without 450nM Cy5-Tm1A was flowed into the glass chamber and allowed to incubate in the dark for 10min. At 10min, a second reaction containing no actin, 150nM hCofilin1 with or without 450nM Cy5-Tm1A was flowed into the chamber, displacing the first reaction. The chamber was then sealed with VALAP and imaged immediately at 10 second intervals.

TIRF with ATP/ADP-actin

To determine whether Tm1A binding to actin filaments formed in the presence of ATP differed from filaments formed in the presence of ADP, we had to create pre-polymerized polarization-marked filaments. To create pre-polymerized polarization-marked filaments, we first incubated a chamber with 1μM streptavidin and 1μM biotin-phalloidin so the actin filaments would be attached to the coverslip. A single filament TIRF reaction with 10% 600nM A488-actin in ATP was flowed into the glass chamber and allowed to incubate in the dark for 5min. Then a reaction with 30% 600nM A488-actin in ATP or ADP was flowed into the glass chamber and allowed to incubate in the dark for 5min. Finally, a reaction with 450nM Cy5-Tm1A in ATP or ADP was flowed into the glass chamber. The chamber was then sealed with VALAP and imaged immediately at 10 second intervals. In this configuration, the pointed ends were dimmer and the barbed ends brighter (Figure S5D). Only filaments that were clearly marked in this manner were chosen for analysis.

Polarized Light Microscopy

Birefringence and fluorescence images were acquired at room temperature on a software-controlled (Micromanager 1.4.15) Nikon Microphot-FXA polarized light microscope equipped with a CRI Abrio camera, and a Nikon 60X (N.A. 1.40) oil immersion objective. Bead motility reactions were started as described above and imaged immediately.

Electron Microscropy

Grids for negative stain were prepared by adding 4ul of 4.5uM Tm1A to carbon-coated grids (Electron Microscopy Sciences 215-412-8400) for 30 seconds. Sample was blotted and grids were washed three times with Tm1A buffer (10mM Imidazole pH 7, 100mM KCl, 0.5mM TCEP). Grids were then stained three times with 0.75% Uranyl Formate and dried. Grids were visualized on a Technai T12 electron microscope at 120kV.

Pyrene Assay

Actin polymerization was measured by monitoring an increase in fluorescence (λ_{ex} = 365nm, λ_{em} = 407nm) of 5%-pyrene-iodoacetamide labeled actin that was purified from rabbit acetone powder. We mixed 10nM Arp2/3, 100nM Arp2/3 activator (ActA$^{30\text{-}612}$-KCK-6XHis) in KMEI (50mM KCl, 1mM $MgCl_2$, 1mM EGTA, 10mM imidazole pH 7.0). Actin polymerization reactions contained 4μM actin (5% pyrene-labeled), all other components were as specified in figure legends. All reaction components, except for actin were mixed in a single tube. Separately, actin was pre-incubated with ME (50μM $MgCl_2$, 20μM EGTA) for 2 minutes, to facilitate the exchange of Ca^{2+} ions for Mg^{2+} ions. Reactions were initiated by addition of actin to the other

components. Time to half max was calculated from the normalized curves by determining the time when a curve crossed 0.5.

Cosedimentation binding assay

AS-Tm1A C32A/S82C (Tm1A) was first diluted to 6.4μM in KMEI and Buffer A. Any aggregates were removed from the Tm1A by centrifugation at 4°C, 227k rcf for 20min. The Tm1A was then diluted serially by 1/2X into KMEI and Buffer A. RSK G-actin was then added to a final concentration of 4μM in KMEI and Buffer A to start the reaction. Since Tm1A can polymerize and sediment on its own, at each concentration of Tm1A, a control reaction was made that did not include actin. Once the reaction was started, a load gel sample was taken immediately, while the binding reactions were allowed to incubate at RT for 2hrs. The reactions were centrifuged at 20°C, 190k rcf for 30min. Gel samples of the supernatant and the pellet were made. All gel samples were made with 250μg/mL BSA as a loading control. Gel samples were run on a NuPAGE 4-12% Bis-Tris gel, stained with Sypro-Red stain (Life Technologies), and imaged on a GE Healthcare Typhoon imager. A titration of actin concentrations was used as a standard. A simple fit of the data was done to determine the Kd and Hill coefficient: bound_ratio(free_TM) = A*(free_TM^Hill/(Kd^Hill + free_TM^Hill)), where A is a constant.

Actin ATP State Growth Simulation

A visual simulation of the ATP state of individual actin subunits in a growing actin filament was developed in MATLAB. These were the conditions and values used:

- Actin monomer size = 6 nm [S15]
- ATP hydrolysis rate = 0.3 1/sec [S16]

- Pi release rate = 0.0062 1/sec [S17]
- BeF_3 Kon rate = $4*10^{-3}$ 1/(μM * sec) [S18]
- ATP-actin growth rate = 11.6 1/(μM * sec) [S19]
- Actin concentration = 0.5 μM
- Time step = 1 sec

Each simulated filament was frozen once it reached a particular length so that the distribution of the different ATP states of the actin subunits could be observed.

Image Analysis

Motility Assay Image Analysis

All image analysis was accomplished with MATLAB code written by the authors. The lengths of the motile actin comet tails were determined by hand-drawn line scans through the middle of the long axis of the tail in each image, using MATLAB code written in-house.

Single Filament TIRF Image Analysis

Tm1A binding distances along single actin filaments was determined by hand-drawn line scans in ImageJ. The hand-drawn kymographs were made in MATLAB where for each filament, a separate line-scan was hand-drawn for every frame. This was necessary because the filaments were not attached to the coverslip.

Analysis for TIRF binding assay

The assumptions for this analysis were: 1) The reaction reached steady-state, and the free monomer pool of actin was equal to the critical concentration of rabbit skeletal muscle actin

(100nM [S20]). Since the concentration of actin added to each reaction was 200nM, the amount of filamentous actin was assumed to be 100nM. 2) The ratio of bound Tm1A to filamentous actin is 1 to 6 [S21]. Putting these assumptions together, the free pool of Tm1A was assumed to be [(concentration of Tm1A added) - 100nM*(# Tm1A pixels on filaments/# actin filament pixels)/6]. To determine the # of pixels in the filaments, each 2-color image was analyzed with MATLAB code written by the authors. The images in each color were converted to binary images with a threshold, skeletonized and the pixels summed. A simple fit of the data was done to determine the Kd and Hill coefficient: bound_ratio(free_TM) = A*(free_TM^Hill/(Kd^Hill + free_TM^Hill)), where A is a constant.

Birefringence Image Analysis

We estimated the order parameter (S) of actin comet tails by computing the ratio between the measured optical retardance —along the slow axis— and the retardance expected for the same density of perfectly aligned filaments [S22]. Comet tails are wider (5 μm) than the Airy disk (~0.3 μm). The retardance measured near the middle of the come tail will, therefore, be proportional to the depth of the network [S23]. The concentration of filamentous actin in our comet tails is ~1 mM [S10], equivalent to a rectangular array of parallel filaments, separated by 0.025 μm. Given a 5 μm-wide comet tail and an Airy disk of 0.3 μm, the number of filaments that contribute to birefringence of is ~1600. If we multiply this number by the retardance of a single actin filament (0.01 nm) we obtain a retardance of ~16 nm for a perfectly aligned comet tail.

Supplemental References

S1. Singh, A., and Hitchcock-DeGregori, S.E. (2007). Tropomyosin's periods are quasi-equivalent for actin binding but have specific regulatory functions. Biochemistry. *46*, 14917-27.

S2. Barua, B., Fagnant, P.M., Windelmann, D.A., Trybus, K.M., and Hitchcock-DeGregori, S.E. (2013). A periodic pattern of evolutionarily conserved basic and acidic residues constitutes the binding interface of actin-tropomyosin. J. Biol. Chem. *288*, 9602-9609.

S3. Li, X.E., Tobacman, L.S., Mun, J.Y., Craig, R., Fischer, S., and Lehman, W. (2011). Tropomyosin position on F-actin revealed by EM reconstruction and computational chemistry. Biophys. J. *100*, 1005-13.

S4. Monteiro, P.B., Lataro, R.C., Ferro, J.A., and Reinach Fde. C. (1994). Function alpha-tropomyosin produced in Escherichia coli. A dipeptide extension can substitute the amino-terminal acetyl group. J. Biol. Chem. *269*, 10461-10466.

S5. Spudich, J.A., and Watt, S. (1971). The regulation of rabbit skeletal muscle contraction. I. Biochemical studies of the interaction of the tropomyosin-troponin complex with actin and the proteolytic fragments of myosin. J. Biol. Chem. *15*, 4866-71.

S6. Cooper, J.A., Walker, S.B., and Pollard, T.D. (1983). Pyrene actin: documentation of the validity of a sensitive assay for actin polymerization. J. Muscle Res. Cell Motil. *4*, 253-262.

S7. Smillie, L.B. (1982). Preparation and identification of alpha- and beta-tropomyosins. Methods Enzymol. *85*, 234–41.

S8. Palmgren, S., Ojala, P.J., Wear, M.A., Cooper, J.A., and Lappalainen, P. (2001). Interactions with PIP2, ADP-actin monomers, and capping protein regulate the activity and localization of yeast twinfilin. J. Cell Biol. *155*, 251-60.

S9. Dayel, M.J., Holleran, E.A., and Mullins, R.D. (2001). Arp2/3 complex requires hydrolyzable ATP for nucleation of new actin filaments. Proc. Nat. Acad. Sci. USA. *98*, 14871-14876.

S10. Akin, O., and Mullins, R.D. (2008). Capping protein increases the rate of actin-based motility by promoting filament nucleation by the Arp2/3 complex. Cell. *133*, 841-851.

S11. Reichstein, E., and Korn, E.D. (1979). Acanthamoeba profilin. A protein of low molecular weight from Acanthamoeba castellanii that inhibits actin nucleation. J. Biol. Chem. *254*, 6174-9.

S12. Carlier, M.F., Laurent, V., Santolini, J., Melki, R., Didry, D., Xia, G.X., Hong, Y., Chua, N.H., and Pantaloni, D. (1997). Actin depolymerizing factor (ADF/cofilin) enhances the rate of filament turnover: implication in actin-based motility. J. Cell Biol. *136*, 1307-1322.

S13. Hand, D.B. (1935). The refractivity of protein solutions. J. Bio. Chem. *108*, 703-707.

S14. Zhao, H. Brown, P.H., Schuck, P. (2011). On the distribution of protein refractive index increments. Biophys. J. *100*, 2309-2317.

S15. Trinick, J., Cooper, J., Seymore, J., and Egelman, E.H. (1986). Cryo-electron microscopy and three-dimensional reconstruction of actin filaments. J. Microsc. *141*, 349-60.

S16. Blanchoin, L., and Pollard, T.D. (2002). Hydrolysis of ATP by polymerized actin depends on the bound divalent cation but not profilin. Biochemistry. *41*, 597-602.

S17. Carlier, M.F. (1987). Measurement of Pi dissociation from actin filaments following ATP hydrolysis using a linked enzyme assay. Biochemical and Biophysical Research Communications. *143*, 1069-1075.

S18. Antonny, B., and Chabre, M. (1992). Characterization of the aluminum and beryllium fluoride species which activate transducin: analysis of the binding and dissociation kinetics. J. Biol. Chem. *267*, 6710-6718.

S19. Pollard, T.D. (1986). Rate constants for the reactions of ATP- and ADP-actin with the ends of actin filaments. J. Cell Biol. *103*, 2747–54.

S20. Fujiwara I., Vavylonis D., Pollard T.D. (2007). Polymerization kinetics of ADP- and ADP-Pi-actin determined by fluorescence microscopy. PNAS. *104*: 8827-32.

S21. Liu Y., Carraway C.A.C., Carraway K.L. (1986). Nonmuscle Tropomyosin from Ascites Tumor Cell Microvilli. J. Biol. Chem. *261*, 4568-73.

S22. de Gennes, P.G. (1974). The physics of liquid crystals (Oxford, UK: Clarendon Press).

S23. LaFountain, J.R., and Oldenbourg, R. (2004). Maloriented bivalents have metaphase positions at the spindle equator with more kinetochore microtubules to one pole than to the other. Molec. Biol. Cell. *15*, 5346-55.